

# Type Ia Supernovae: Influence of the Progenitor on the Explosion

INMA DOMÍNGUEZ<sup>1</sup>, PETER HÖFLICH<sup>2,3</sup>, OSCAR STRANIERO<sup>4</sup> CRAIG WHEELER<sup>2</sup>,  
FRIEDRICH-KARL THIELEMANN<sup>3</sup>

<sup>1</sup> *Universidad de Granada, Granada, Spain*

<sup>2</sup> *University of Texas, Austin, USA*

<sup>3</sup> *University of Basel, Basel, Switzerland*

<sup>4</sup> *Osservatorio Astronomico di Collurania, Teramo, Italy*

**Abstract.** The influence of the initial composition and structure of the exploding white dwarf on the nucleosynthesis and structure of Type Ia Supernovae has been studied. The progenitor structures are based on detailed stellar evolutionary tracks for stars in the mass range between 1 to 9  $M_{\odot}$  using the state of the art code FRANEC. The calculations of the thermonuclear explosions are based on a set of delayed detonation models which give a good account of the optical and infrared light curves and of the spectral evolution. Our code solves the hydrodynamical equations explicitly by the piecewise parabolic method. Nuclear burning is taken into account using an extended network of 218 nuclei. In principle, our calculations allow the observed spectra and light curve to be linked to the progenitor. Moreover, our study is relevant to estimate potential evolution in the progenitor population at cosmological time scales.

## 1 Explosion Models

The influence of initial metallicity and C/O ratio on the light curves and spectra has been studied for a set of delayed detonation models. The explosions are calculated using a one dimensional radiation-hydro code, including nuclear network ([11] and references therein). For all the models, the WD mass is  $1.4M_{\odot}$ , the central density of the WD is  $2.6 \times 10^9$  g/cm<sup>3</sup> and the ratio of the deflagration velocity to the local sound speed is 0.03. Table 1 shows basic parameters for the delayed detonation models: these are, from column 2 to 6, transition density (in g/cm<sup>3</sup>), at which the deflagration is assumed to turn into a detonation, metallicity relative to solar, C/O ratio, kinetic energy (in erg) and mass of  $^{56}\text{Ni}$  (in solar units). The identification for the selected models is shown in column 1, with DD21c being the reference model.

**Table 1.** Delayed Detonation Models

Model	$\rho_{tr}$	$Z/Z_{\odot}$	C/O	$E_{kin}$	$M_{Ni}$
<b>DD21c</b>	$2.7 \times 10^7$	1.0	1.0	$1.32 \times 10^{51}$	0.69
DD23c	$2.7 \times 10^7$	1.0	<b>0.66</b>	$1.18 \times 10^{51}$	0.59
DD24c	$2.7 \times 10^7$	<b>1/3</b>	1.0	$1.32 \times 10^{51}$	0.70
DD13c	<b><math>3.0 \times 10^7</math></b>	1.0	1.0	$1.36 \times 10^{51}$	0.79

The corresponding bolometric light curves have been calculated ([10] and references therein). A decrease in C implies a decrease in  $^{56}\text{Ni}$  and consequently a decrease in the luminosity at later times (instantaneous deposition of the radioactive energy). However, the maximum luminosity is greater because the smaller kinetic energy causes a lower expansion rate and more of the stored energy contributes to the luminosity.

Both effects cause a steeper decline rate after maximum light. Moreover if C is decreased, the energy release during nuclear burning is also lowered and the transition density is reached later, resulting in a larger pre-expansion of the outer layers. In a first approximation, this is equivalent to a reduction of the transition density. Lower expansion velocities and a narrower region dominated by Si are obtained in both cases.

The bolometric and monochromatic light curves are rather insensitive to the changes in metallicity. As shown in Table 1, both the  $^{56}\text{Ni}$  mass and the kinetic energy are close to the values obtained for the *reference* model, DD21c. Synthetic NLTE spectra are calculated ([9], [10] and references therein). The changes due to different metallicities can be directly observed in the UV spectral region. Lower metallicities and thus higher  $Y_e$  produce less  $^{54}\text{Fe}$  [13], which provides an important source for the opacity. However, this will only affect external regions (with  $v_{exp}$  above 12000 km/s); Moreover 2 or 3 weeks after maximum when the spectrum is formed in the inner regions it becomes insensitive to the initial metallicity of the WD.

## 2 Evolutionary Models

Evolutionary tracks for a full set of intermediate mass star models have been obtained using the code FRANEC [19] and [7]. A full description of the updated input physics can be found in [18]. The main problem related to the evolution of intermediate mass stars is the treatment of turbulent convection. In this work the extension of the convective regions is fixed by the Schwarzschild criterion (without mechanical overshooting). Semiconvection during central helium burning is included, while the *breathing pulses* at the end of the central He burning phase are inhibited.

The main results are illustrated in Table 2, where columns 1 to 9 show, respectively, the main sequence mass (in solar units), the initial metallicity and helium, the mass of the C-O core at the thermal pulse phase (in solar units), the central mass fraction of C, the C/O ratio within the core, the C/O ratio after attaining the Chandrasekhar mass (for the accreted matter C/O=1 is assumed), the source of the  $^{12}\text{C}(\alpha, \gamma)^{16}\text{O}$  rate: CF85 corresponds to Caughlan and Fowler [4], B-H96 and B-L96 to the upper and lower limits according to Buchmann [2] and [3] and the numbers of thermal pulses calculated. Note that the C-O core chemical structure is taken at the last thermal pulse.

The amount of C decreases as the WD progenitor mass increases or WD progenitor metallicity decreases (see Table 2). The maximum difference obtained, once the C-O core is accreted to the Chandrasekhar mass, is about 18% (see Table 2 and Figure 1) for the maximum difference in progenitor masses and about 5% for the maximum difference in progenitor metallicity (see Table 2 and Figure 2 *left*).

The assumed  $^{12}\text{C}(\alpha, \gamma)^{16}\text{O}$  reaction rate constitutes a critical point (see Table 2 and Figure 2 *right*). When central helium is depleted to 0.1 (mass fraction) the burning mainly occurs through this reaction, determining the  $^{12}\text{C}/^{16}\text{O}$  profile in the final WD. However, note that the adoption of a particular rate should be done in accordance with the decision of the convection criterion. The treatment of convection in our code is consistent with a *high* reaction rate.

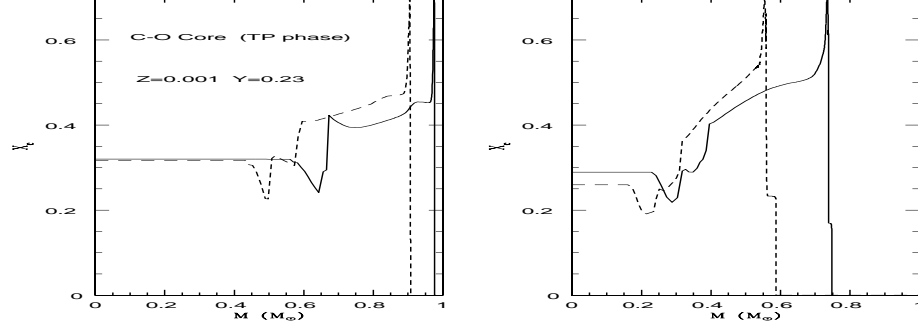


Figure 1: Carbon abundance (mass fraction) in the C-O core for the selected masses ( $Z=0.001$  and  $Y=0.23$ ). *left*:  $6M_{\odot}$  (solid) and  $5M_{\odot}$  (dashed). *right*:  $3M_{\odot}$  (solid) and  $1.5M_{\odot}$  (dashed).

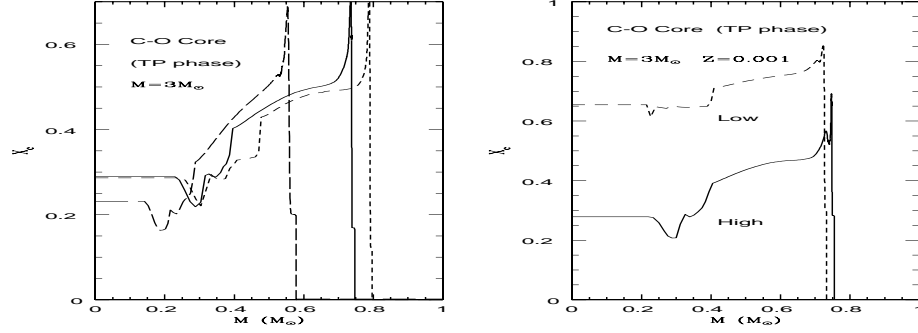


Figure 2: Carbon abundance (mass fraction) in the C-O core. *left*: Models with different metallicities ( $3M_{\odot}$ ):  $Z=0.0001$ ,  $Y=0.23$  (short dashed),  $Z=0.001$ ,  $Y=0.23$  (solid) and  $Z=0.02$ ,  $Y=0.28$  (long dashed). *right*: The high and low rates for the  $^{12}\text{C}(\alpha, \gamma)^{16}\text{O}$  proposed by L. Buchmann (1996, 1997) are adopted ( $M=3M_{\odot}$ ,  $Z=0.001$  and  $Y=0.23$ ).

**Table 2.** Properties of the CO core at the TP-AGB phase

$M_T$	$Z$	$Y$	$M_{CO}$	$C_C$	$C/O_{core}$	$C/O_{Mch}$	Rate	TP (number)
1.5	0.001	0.23	0.560	0.260	0.533	0.781	CF85	3
<b>3.0</b>	0.001	0.23	<b>0.738</b>	<b>0.289</b>	<b>0.610</b>	<b>0.772</b>	CF85	2
5.0	0.001	0.23	0.907	0.316	0.563	0.691	CF85	1
6.0	0.001	0.23	0.976	0.320	0.537	0.650	CF85	1
3.0	0.0001	0.23	0.791	0.286	0.587	0.741	CF85	1
3.0	0.001	0.28	0.815	0.297	0.623	0.760	CF85	8
3.0	0.02	0.28	0.561	0.232	0.522	0.778	CF85	3
3.0	0.001	0.23	0.750	0.279	0.570	0.742	B-H96	6
3.0	0.001	0.23	0.727	0.654	2.314	1.525	B-L96	5
3.0	0.001	0.23	0.759	0.289	0.621	0.773	CF85	11

### 3 Supernovae at High Redshifts and Cosmology.

The successful detection of SNe Ia at high redshifts, currently around 96 SNe with redshifts ranging from 0.18 to 0.86 [14], [15], [16] and [17], has provided an exciting new tool for cosmology research. An astonishing conclusion has been reached: results are consistent with a low matter density universe and a positive cosmological constant. These results are based on two assumptions: that SNe Ia are nearly standard candles and that individual deviations can be detected using a local calibration of the brightness-decline relation.

However, several observations indicate the presence of evolutionary effects: SNe Ia are dimmer in elliptical galaxies and in the outer regions of spirals; in the central region of spirals, both intrinsically brighter and dimmer SNe Ia occur, while they are relatively underrepresented in the bulges of spiral galaxies [1], [8] and [21].

Time evolution is expected to produce several effects (see [10] and [6] for a complete description). The most important effects directly related to this study concern the progenitor mass and metallicity. At early epochs the mean progenitor mass is larger and a smaller C/O is expected (see Table 2). A smaller C/O increases the peak-to-tail luminosity ratio. Moreover, the C/O ratio influences the ignition conditions and the propagation of the burning front. The initial metallicity determines the electron-nucleon fraction of the outer layers and hence affects the products of nuclear burning. The changes in the spectrum with changes in metallicity have an important effect on the colours of SNe Ia at high redshifts, where they are shifted into other bands.

We obtained evolutionary effects of the order of 0.15 to 0.3 mag [10] and [6], due to changes in the brightness-decline relation and in the spectra. These effects are small but are of the same order as the brightness change (0.15 mag) imposed by cosmological deceleration.

### References

- [1] Branch D., Romanishin W., Baron E. 1996, ApJ 465, 73; erratum 467, 473
- [2] Buchmann L. 1996, ApJ 468, L127
- [3] Buchmann L. 1997, ApJ 479, L153
- [4] Caughlan G.R., Fowler A.M. 1985, ARA&A, 21, 165
- [5] Chieffi A. and Straniero O. 1989, ApJ 71, 47
- [6] Dominguez I., Höflich P., Wheeler J.C., Straniero O. 1998, ApJ, in preparation
- [7] Dominguez I., Straniero O., Chieffi A., Limongi M. 1998, ApJSS, in preparation
- [8] Hamuy M., Phillips M.M., Maza J., Suntzeff N.B., Schommer R.A., Aviles A. 1996, ApJ 112, 2438
- [9] Höflich, P. 1995, ApJ, 443, 89
- [10] Höflich P., Wheeler J.C., Thielemann F.K. 1998, ApJ, 495, 617
- [11] Höflich P., Khokhlov A. 1996, ApJ, 457, 500
- [12] Höflich P., Khokhlov A., Wheeler J.C. 1995, ApJ, 444, 211
- [13] Nomoto K., Thielemann F.-K., Yokoi K. 1984, ApJ, 286, 644
- [14] Perlmutter C. et al. 1995, ApJ Lett, 440, 95
- [15] Perlmutter C. et al. 1997, ApJ, 483, 565
- [16] Riess A.G., Press W.H., Kirshner R.P. 1995, ApJ, 438, L17
- [17] Riess A.G., et al. 1998, ApJ, in press
- [18] Straniero, O., Chieffi, A. and Limongi M. 1997 ApJ, 490, 425
- [19] Straniero, O., Chieffi, A., Limongi M., Dominguez, I. 1998 in *Views on Distance Indicators*, Mem. S.A.I., Ed. F. Caputo, in press
- [20] Thielemann F.K., Nomoto K., Hashimoto M. 1996, ApJ, 460, 408
- [21] Wang L., Höflich P., Wheeler J.C., 1997, ApJ, 483, 29